

The extraction of light cone parton distributions from lattice quantum chromodynamics

Savvas Zafeiropoulos
HadStruc Collaboration

CPT, Marseille

07.06.2023

Hadron 2023, Genoa

In collaboration with P. Barry (JLAB), L. DelDebbio (Edinburgh), R. Edwards (JLAB), C. Egerer (JLAB), T. Giani (NIKHEF), B. Joo (ORNL), J. Karpie (JLAB), N. Karthik (APS), T. Khan (Brac U.), W. Melnitchouk (JLAB), K. Orginos (College of William & Mary and JLAB), A. Radyushkin (ODU and JLAB), D. Richards (JLAB), E. Romero (JLAB), A. Rothkopf (Stavanger U.), N. Sato (JLAB), R. Sufian (BNL)

PDFs are of paramount importance because...

- The uncertainties in PDFs are the **dominant theoretical uncertainties** in Higgs couplings, α_s and the mass of the W boson

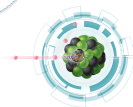
- Beyond the LHC, PDFs play an important role, for instance in astroparticle physics, such as for the accurate predictions for signal and background events at ultra-high energy neutrino telescopes (ANITA, IceCube, Pierre Auger Observatory)



Future Circular Collider
Circumference: 80-100 km
Energy: 100 TeV (pp)
>350 GeV (e^+e^-)

Large Hadron Collider
Circumference: 27 km
Energy: 14 TeV (pp)
209 GeV (e^+e^-)

Tevatron (closed)
Circumference: 6.2 km
Energy: 2 TeV

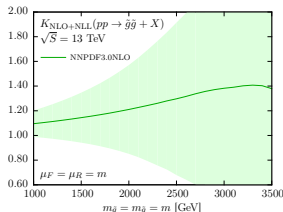
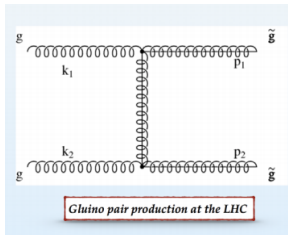



- PDFs will keep playing an important role for any future high energy collider involving hadrons in the initial state. Therefore improving our understanding of PDFs also strengthens the physics potential of such future colliders

 Gao, Harland-Lang, Rojo (2018)

PDF uncertainties and BSM Physics

The uncertainty on the PDFs is rapidly becoming one of the limiting factors in searches for new physics.



The relative size of the NLL corrections for gluino pair production was computed. The error in the relative size of the NLL corrections grows very quickly as the gluino mass is increased, mostly as a consequence of the large PDF errors at large values of x .  Beenakker et al. (2016)

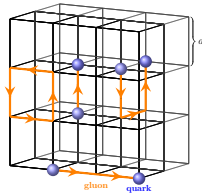
From DIS to PDFs via factorization

- The measurement of PDFs is made possible due to factorization theorems
- Intuitively, factorization theorems tell us that the same universal non-perturbative objects (the PDFs), representing long distance physics, can be combined with many short-distance calculations in QCD to give the cross-sections of various processes

$$\sigma = f \otimes H$$

- ▶ f are the PDFs, H is the hard perturbative part and \otimes is convolution.
- ▶ PDFs truly characterize the hadronic target
- ▶ PDFs are essentially non-perturbative

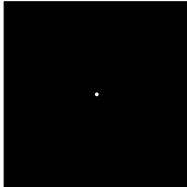
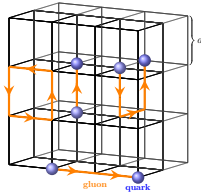
Lattice?



- The natural ab-initio method to study QCD non-perturbatively is on the lattice. But ...
- PDFs are defined as an expectation value of a bilocal operator evaluated along a light-like line.
- Clearly, we can not evaluate this on a Euclidean set-up.



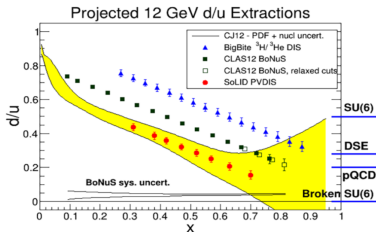
Lattice?



- The natural ab-initio method to study QCD non-perturbatively is on the lattice. But ...
- PDFs are defined as an expectation value of a bilocal operator evaluated along a light-like line.
- Clearly, we can not evaluate this on a Euclidean set-up.

Large- x discrepancies for the nucleon and the pion

The nucleon



- JLab 12-GeV measurements of the ratio of the PDFs for the d and u quarks at large momentum fraction x
- In yellow the projected uncertainty in measurements under several theoretical assumptions

The pion

Model/theory	large x
QCD parton model	$(1-x)^2$
pQCD	$(1-x)^{2+\gamma}$
Light-front holographic QCD	$(1-x)^0$
Nambu-Jona-Lasino/duality	$(1-x)^1$

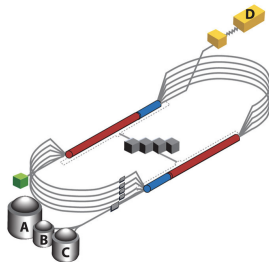
- \bar{u} quark distribution of π^- extracted @FNAL E615
- Large- x of pion PDF is the goal @JLab-C12-15-006, @COMPASS-CERN. Large- x of kaon PDF is the goal @JLab-C12-15-006A

An ab-initio non-perturbative QCD calculation is timely and imperative!

Experimental Research Facilities



Experimental Research Facilities




JLAB 12 GeV upgrade

Experimental Research Facilities

The Electron-Ion Collider

A machine that will unlock the secrets of the strongest force in Nature



The computers and smartphones we use every day depend on what we learned about the atom in the last century. All information technology—and much of our economy today—relies on understanding the electromagnetic force between the atomic nucleus and the electrons that orbit it. The science of that force is well understood but we still know little about the microcosm within the protons and neutrons that make up the atomic nucleus. That's why Brookhaven Lab is building a new machine—an Electron-Ion Collider, or EIC—to look *inside* the nucleus and its protons and neutrons.


The EIC will be a particle accelerator that collides electrons with protons and nuclei to produce snapshots of those particles' internal structure—like a CT scanner for atoms. The electron beam will reveal the arrangement of the quarks and gluons that make up the protons and neutrons of nuclei. The force that holds quarks together, carried by the gluons, is the strongest force in Nature. The EIC will allow us to study this "strong nuclear force" and the role of gluons in the matter within and all around us. What we learn from the EIC could power the technologies of tomorrow.

taken from <https://www.bnl.gov/eic/>

The Ji Idea

- Lattice QCD computes equal time matrix elements
- Displace quarks in space-like interval
- Boost states to “infinite” momentum
- On the frame of the proton displacement becomes lightlike
- But infinite momentum not possible on the lattice
- Use perturbative matching from finite momentum [X. Ji \(2013\)](#)
- One needs to deal with the divergences

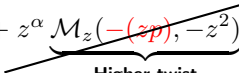
PDFs from the lattice: Pseudo-PDFs Formalism



Starting point: the equal time hadronic matrix element with the quark and anti-quark fields separated by a finite distance  Radyushkin (2017)

$$\mathcal{M}^\alpha(z, p) \equiv \langle p | \bar{\psi}(0) \gamma^\alpha \hat{E}(0, z; A) \tau_3 \psi(z) | p \rangle$$

$z = (0, 0, 0, z_3)$
 $p = (p^0, 0, 0, p)$
 $\alpha = 0$

Lorentz inv. \rightarrow

$$\mathcal{M}^\alpha(z, p) = 2p^\alpha \underbrace{\mathcal{M}_p(-\textcolor{red}{zp}), -z^2}_{\text{Leading twist}} + z^\alpha \underbrace{\mathcal{M}_z(-\textcolor{red}{zp}), -z^2}_{\text{Higher twist}}$$



- The Lorentz invariant quantity $\nu = -\textcolor{red}{zp}$, is the "loffe time"
- loffe time PDFs $\mathcal{M}(\nu, z_3^2)$ defined at a scale $\mu^2 = 4e^{-2\gamma_E}/z_3^2$ (at leading log level) are the Fourier transform of regular PDFs $f(x, \mu^2)$  Balitsky, Braun (1988),  Braun et al. (1995)

$$\mathcal{M}(\nu, z_3^2) = \int_{-1}^1 dx f(x, 1/z_3^2) e^{i x \nu}$$

Obtaining the Ioffe time PDF

$$z_3 \rightarrow 0 \Rightarrow \mathcal{M}_p(\nu, z_3^2) = \mathcal{M}(\nu, z_3^2) + \mathcal{O}(z_3^2)$$

But.... large $\mathcal{O}(z_3^2)$ corrections **prohibit** the extraction.

In a **ratio** z_3^2 corrections might cancel  Radyushkin (2017)

$$\mathfrak{M}(\nu, z_3^2) \equiv \frac{\mathcal{M}_p(\nu, z_3^2)}{\mathcal{M}_p(0, z_3^2)}$$

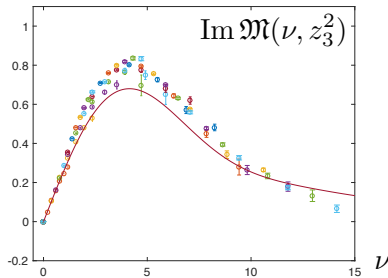
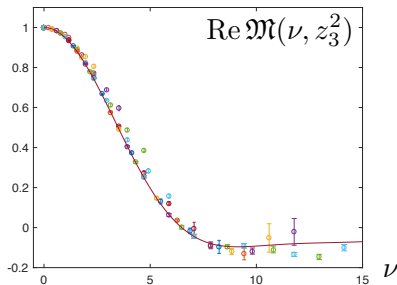
- Much **smaller** $\mathcal{O}(z_3^2)$ corrections and therefore this ratio could be used to extract the Ioffe time PDFs
- All UV singularities are **exactly cancelled** and when computed in lattice QCD it can be extrapolated to the continuum limit

■

$$\mathfrak{M}(\nu, z^2) = \int_0^1 d\alpha \mathcal{C}(\alpha, z^2 \mu^2, \alpha_s(\mu)) \mathcal{Q}(\alpha \nu, \mu) + \sum_{k=1}^{\infty} \mathcal{B}_k(\nu) (z^2)^k,$$

μ is the factorization scale and $\mathcal{Q}(\nu, \mu)$ is the Ioffe time PDF

Results for the Re and Im parts of $\mathfrak{M}(\nu, z_3^2)$



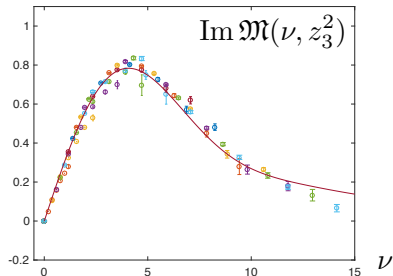
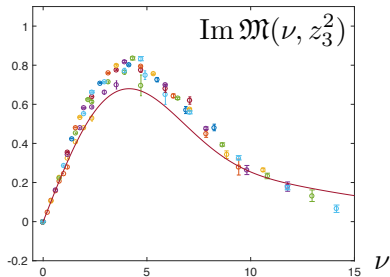
- First case study in an unphysical setup [Karpie, Orginos, Radyushkin SZ, Phys.Rev. D96 \(2017\) no.9, 094503](#)

Curves represent Re and Im Fourier transforms of $q_v(x) = \frac{315}{32} \sqrt{x}(1-x)^3$.

- Considering CP even and odd combinations

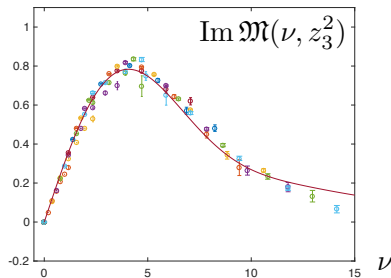
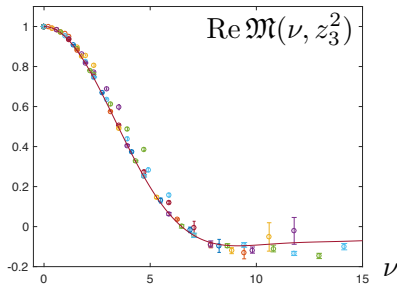
- ▶ even: $q_-(x) = f(x) + f(-x) = q(x) - \bar{q}(x) = q_v(x)$
- ▶ odd: $q_+(x) = f(x) - f(-x) = q(x) + \bar{q}(x) = q_v(x) + 2\bar{q}(x)$

Results for the Im part of $\mathfrak{M}(\nu, z_3^2)$



- Curves represent the Im Fourier transforms of $q_v(x) = q(x) - \bar{q}(x)$ and $q_+(x) = q(x) + \bar{q}(x) = q_v(x) + 2\bar{q}(x)$ respectively.
- The agreement with the data is strongly improved if we use a non-vanishing antiquark contribution, namely $\bar{q}(x) = \bar{u}(x) + \bar{d}(x) = 0.07[20x(1-x)^3]$.

Results for the Re and Im parts of $\mathfrak{M}(\nu, z_3^2)$



- Data as function of the loffe time. A **residual** z_3 -dependence can be seen.
- This is more visible when, for a **particular** ν we have several data points corresponding to **different values of** z_3 .
- Different values of z_3^2 for the same ν correspond to the loffe time distribution at different scales.

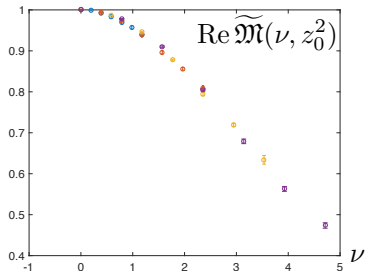
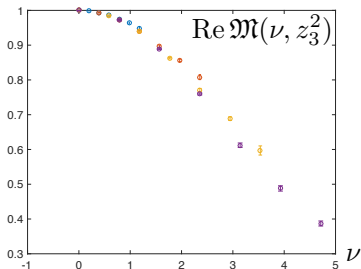
Residual z_3 -dependence

- Is the residual scatter in the data points **consistent with evolution**? By solving the evolution equation at LO, the loffe time PDF at z'_3 is related to the one at z_3 by

$$\mathfrak{M}(\nu, z'^2_3) = \mathfrak{M}(\nu, z^2_3) - \frac{2}{3} \frac{\alpha_s}{\pi} \ln(z'^2_3 / z^2_3) \int_0^1 du B(u) \mathfrak{M}(u\nu, z^2_3)$$

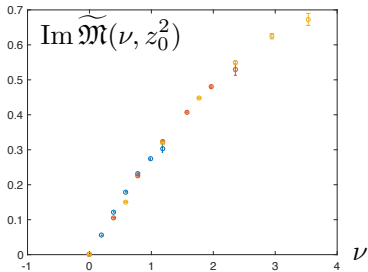
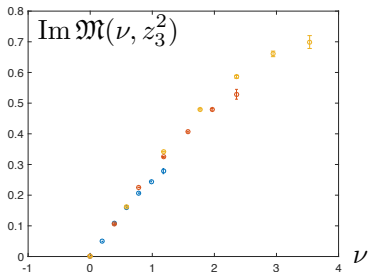
- Only applicable at small z_3
- Check its effect using data at values of $z_3 \leq 4a$ corresponding to energy scales larger than 500 MeV.
- We fix the point z'_3 at the value $z_0 = 2a$ corresponding, at leading logarithm level, to the $\overline{\text{MS}}$ -scheme scale $\mu_0 = 1$ GeV and evolve the rest of the points to that scale.

Before and after evolution



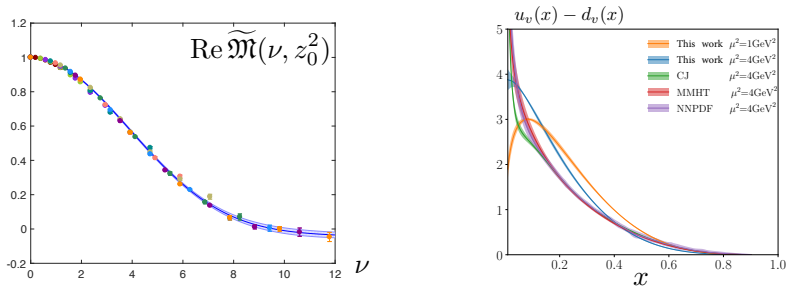
The ratio $\mathfrak{M}(\nu, z_3^2)$ for $z_3/a = 1, 2, 3$, and 4. **LHS:** Data **before evolution**. **RHS:** Data **after evolution**. The reduction in scatter indicates that evolution collapses all data to the same universal curve.

Before and after evolution



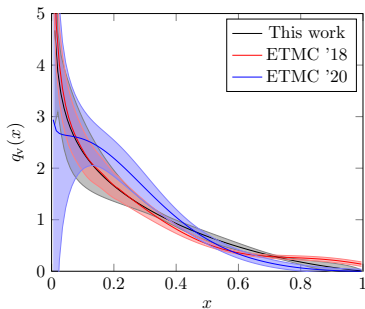
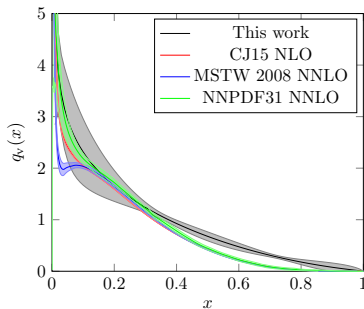
The ratio $\mathfrak{M}(\nu, z_3^2)$ for $z_3/a = 1, 2, 3$, and 4. **LHS:** Data **before evolution**. **RHS:** Data **after evolution**. The reduction in scatter indicates that evolution collapses all data to the same universal curve.

Comparisons with global fits



Left: Data points for $\text{Re } \widetilde{\mathcal{M}}(\nu, z_3^2)$ with $z_3 \leq 10a$ evolved to $z_3 = 2a$ as described in the text. Right: Curve for $u_v(x) - d_v(x)$ built from the evolved data shown in the left panel and treated as corresponding to the $\mu^2 = 1 \text{ GeV}^2$ scale; then evolved to the reference point $\mu^2 = 4 \text{ GeV}^2$ of the global fits.


New results with $N_f = 2 + 1$ fermions for the nucleon



Our determination of the phys. pion mass nucleon valence PDF compared to pheno and other lattice determinations. [Joo, Karpie, Orginos, Radyushkin, Richards, S.Z.](#)

Phys.Rev.Lett. 125 (2020) 23, 232003

The Continuum and Leading Twist Limits of Parton Distribution Functions in Lattice QCD

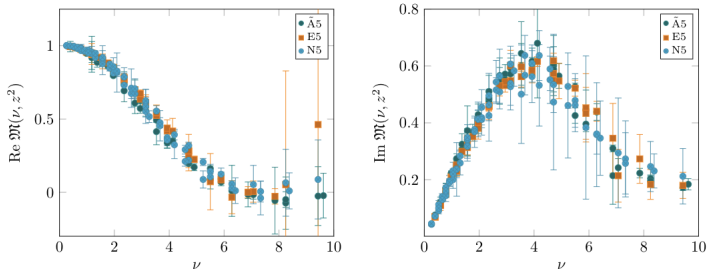
- In  Karpie, Orginos, Radyushkin and S.Z. JHEP 11 (2021) 024 we present continuum limit results
- first continuum limit using the pseudo-PDF approach with Short Distance Factorization for factorizing lattice QCD calculable matrix elements
- we are employing the summation Generalized Eigenvalue Problem (sGEVP) technique in order to optimize our control over the excited state contamination which can be one of the most serious systematic errors in this type of calculations
- crucial novel ingredient of our analysis is the parameterization of systematic errors using Jacobi polynomials to characterize and remove both lattice spacing and higher twist contaminations, as well as the leading twist distribution
- method can be expanded in further studies to remove all other systematic errors

The Continuum and Leading Twist Limits of Parton Distribution Functions in Lattice QCD

ID	$a(\text{fm})$	$M_\pi(\text{MeV})$	β	c_{SW}	κ	$L^3 \times T$	N_{cfg}
$\tilde{A}5$	0.0749(8)	446(1)	5.2	2.01715	0.13585	$32^3 \times 64$	1904
E5	0.0652(6)	440(5)	5.3	1.90952	0.13625	$32^3 \times 64$	999
N5	0.0483(4)	443(4)	5.5	1.75150	0.13660	$48^3 \times 96$	477

Parameters for the lattices generated by the CLS collaboration using two flavors of $\mathcal{O}(a)$ improved Wilson fermions.

The Continuum and Leading Twist Limits of Parton Distribution Functions in Lattice QCD



The real (LHS) and the imaginary (RHS) part of the reduced ITDs of the three lattice ensembles used in this study. We see that for the range of loffe times that is covered by our data the three ensembles have a pretty good overlap. The statistical and systematic errors are added in quadrature.

The Continuum and Leading Twist Limits of Parton Distribution Functions in Lattice QCD

A Taylor expansion in lattice spacing gives the continuum reduced pseudo-ITD $\mathfrak{M}_{\text{cont}}$ and lattice spacing corrections

$$\mathfrak{M}(p, z, a) = \mathfrak{M}_{\text{cont}}(\nu, z^2) + \sum_{n=1} \left(\frac{a}{|z|} \right)^n P_n(\nu) + (a\Lambda_{\text{QCD}})^n R_n(\nu)$$

With an $O(a)$ improved lattice action, the lattice spacing errors related to the momentum p , must come in from the momentum transfer. This feature is known in the improvement of the local vector current. The higher twist power corrections are added as nuisance terms similar to the lattice spacing terms. The functional form is given by

$$\mathfrak{M}_{\text{cont}}(\nu, z^2) = \mathfrak{M}_{\text{lt}}(\nu, z^2) + \sum_{n=1} (z^2 \Lambda_{\text{QCD}}^2)^n B_n(\nu).$$

The Continuum and Leading Twist Limits of Parton Distribution Functions in Lattice QCD

All of the unknown functions, $q_-(x)$, $q_+(x)$, $P_1(\nu)$, $R_1(\nu)$, and $B_1(\nu)$, are parameterized using Jacobi polynomials.

The Jacobi polynomials, $j_n^{(\alpha,\beta)}(z)$, are defined in the interval $[-1, 1]$ and they satisfy the orthogonality relation

$$\int_{-1}^1 dz (1-z)^\alpha (1+z)^\beta j_n^{(\alpha,\beta)}(z) j_m^{(\alpha,\beta)}(z) = \tilde{N}_n^{(\alpha,\beta)} \delta_{n,m} ,$$

for $\alpha, \beta > -1$. COV $x = \frac{1-z}{2}$ or $z = 1 - 2x$. This transformation maps the interval $[-1, 1]$ to the interval $[0, 1]$ and the orthogonality weight becomes $(1-z)^\alpha (1+z)^\beta = 2^{\alpha+\beta} x^\alpha (1-x)^\beta$. We then introduce the transformed Jacobi polynomials $J_n^{(\alpha,\beta)}(x)$, as

$$J_n^{(\alpha,\beta)}(x) = \sum_{j=0}^n \omega_{n,j}^{(\alpha,\beta)} x^j .$$

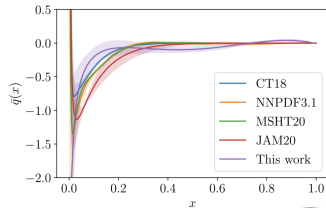
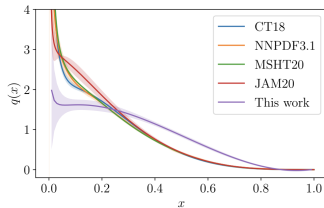
The Continuum and Leading Twist Limits of PDFs

Since the Jacobi polynomials form a complete basis of functions in the interval of $[0,1]$, the PDFs can be written as

$$q_{\pm}(x) = x^{\alpha}(1-x)^{\beta} \sum_{n=0}^{\infty} \pm d_n^{(\alpha,\beta)} J_n^{(\alpha,\beta)}(x)$$

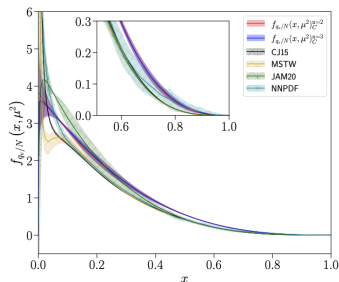
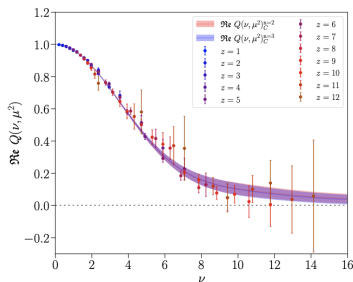
for any α and β . The choice of those parameters does affect the convergence of the coefficients $\pm d_n^{(\alpha,\beta)}$. One needs to truncate the series introducing in this way some model dependence which can be easily controlled. The control of the truncation can be improved if one fits for the optimal values of α and β for that given order of truncation. In other words, the rate of convergence of the series can be optimized by tuning the values of α and β .

The Continuum and Leading Twist Limits of PDFs



Isvector quark and anti-quark distributions-comparing to phenomenology

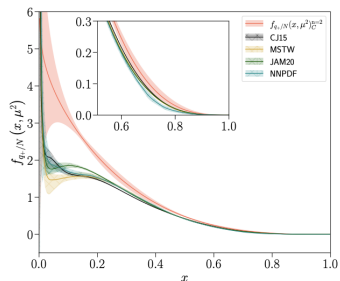
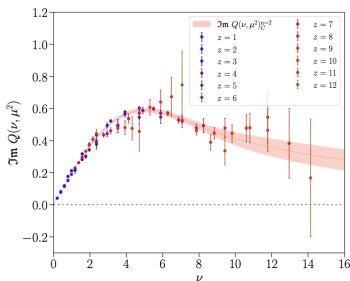
Towards High-Precision Parton Distributions From Lattice QCD via Distillation



The real component of the matched ITD at $\mu = 2$ GeV in $\overline{\text{MS}}$ fit by cosine transforms of two- and three-parameter model PDFs. The nucleon unpolarized valence quark PDF at 2 GeV in $\overline{\text{MS}}$ determined from the uncorrelated cosine transform fits applied to real component of the matched ITD. Comparisons are made with the NLO global analyses of CJ15 and JAM20, and the NNLO analyses of MSTW and NNPDF at the same scale.

 Egerer, Edwards, Kallidonis, Orginos, Radyushkin, Richards, Romero and S.Z. JHEP11(2021)148

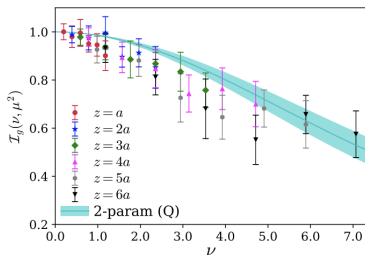
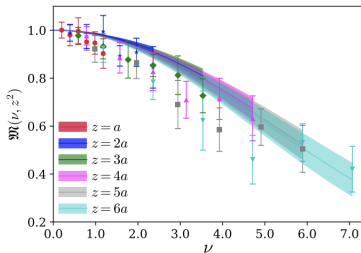
Towards High-Precision Parton Distributions From Lattice QCD via Distillation



The imaginary component of the matched ITD at $\mu = 2$ GeV in $\overline{\text{MS}}$ fit by the sine transform of a two-parameter model PDF. Data has been fit for $z/a \leq 12$, and correlations have been neglected. The nucleon unpolarized plus quark PDF at 2 GeV in $\overline{\text{MS}}$ determined from the uncorrelated sine transform fits applied to the imaginary component of the matched ITD. Comparisons are made with the NLO global analyses of CJ15 and JAM20, and the NNLO analyses of MSTW and NNPDF at the same scale. [Egerer,](#)

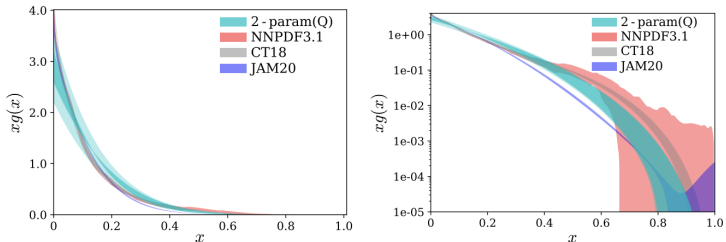
Edwards, Kallidonis, Orginos, Radyushkin, Richards, Romero and S.Z. JHEP11(2021)148

Gluon PDF



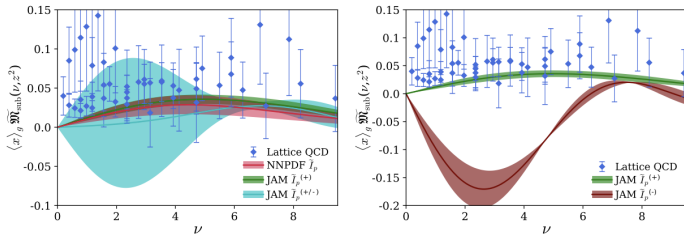
🔗 Khan, Sufian, Karpie, Monahan, Egerer, Joo, Morris, Orginos, Radyushkin, Richards, Romero and S.Z. Phys.Rev.D 104 (2021) 9, 094516 Lattice reduced pseudo-ITD shown along with their reconstructed fitted bands and the $\overline{\text{MS}}$ matched ITD at 2GeV.

Gluon PDF



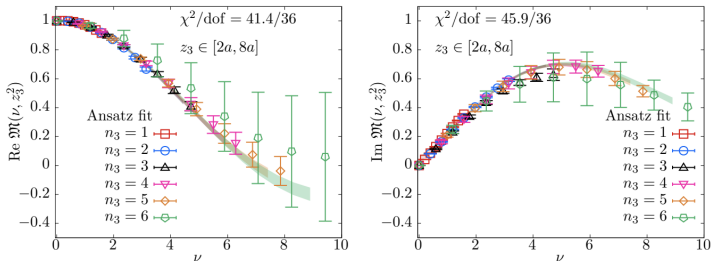
[Khan, Sufian, Karpie, Monahan, Egerer, Joo, Morris, Orginos, Radyushkin, Richards, Romero and S.Z. Phys.Rev.D 104 \(2021\) 9, 094516](#) Unpolarized gluon PDF (cyan band) extracted from our lattice data using the 2-param (Q) model. We compare our results to gluon PDFs extracted from global fits to experimental data, CT18, NNPDF3.1, and JAM20. Normalization of the gluon PDF using the gluon momentum fraction $\langle x \rangle_g^{\overline{MS}}(\mu = 2 \text{ GeV}) = 0.427(92)$ from [Alexandrou et al Phys.Rev.D 101 \(2020\) 9, 094513](#). On the L/RHS the same distributions with different scales for $x g(x)$ to enhance the view of the large- x region.


Gluon helicity distribution



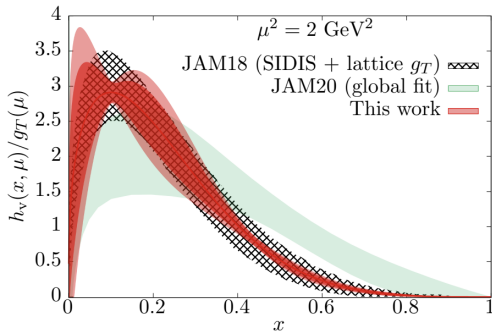
✍ Egerer, Joo, Karpie, Karthik, Khan, Monahan, Morris, Orginos, Radyushkin, Richards, Romero, Sufian and S.Z, Phys.Rev.D 106 (2022) 9, 094511 The lattice reduced pITD in the zero flow-time limit obtained through the subtraction method using the $p = 0$ matrix elements, and the gluon helicity ITD constructed from global fits. In the LHS the red band denotes the ITD constructed from the gluon helicity distribution by the NNPDF collaboration. The green band and the cyan band represent the gluon helicity ITD determined by the JAM collaboration with and without the positivity constraint. The green band and the maroon band represent the gluon helicity ITD determined by the JAM collaboration associated with the positive and negative gluon helicity PDF solutions.

Transversity PDF



 Egerer, Kallidonis, Karpie, Karthik, Morris, Orginos, Radyushkin, Romero, Sufian and S.Z. Phys.Rev.D 105 (2022) 3, 034507 Reconstruction of transversity PDF based on a “Jam Ansatz”. The real and imaginary parts of \mathfrak{M} are shown as a function of ν . They show the best fit bands resulting from an analysis assuming the PDF ansatz. The fits shown in the figure incorporated the data points at all momenta with $z_3 \in [2a, 8a]$. The color of the bands and the data points distinguish the fixed value of momenta $P_3 = 0.41n_3$ GeV used.

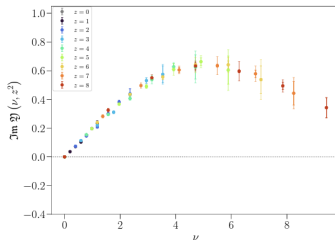
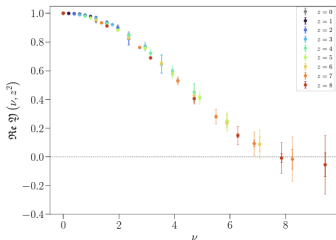
Transversity PDF



[Egerer, Kallidonis, Karpie, Karthik, Morris, Orginos, Radyushkin, Romero, Sufian and S.Z. Phys.Rev.D 105 \(2022\) 3,](#)

034507 The valence transversity distribution $h_v(x, \mu)/g_T(\mu)$. The inner red band includes only the statistical error and the outer red band includes statistical and systematical errors in the PDF reconstruction. Comparison is made with the previous phenomenological determinations using SIDIS and lattice g_T (JAM18), shown using a patterned band, and with the recently updated global fit analysis (JAM20) of the single transverse spin asymmetry data (but, without including lattice g_T), shown as a green band.

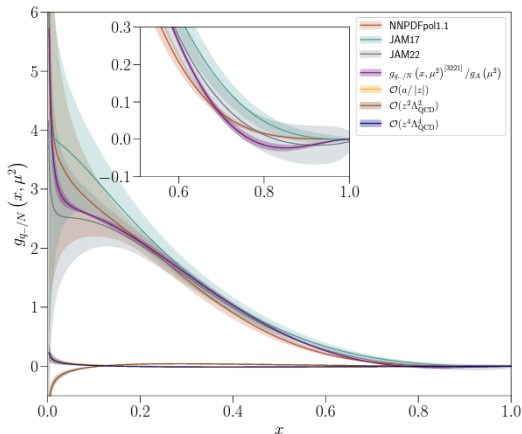
Helicity PDF




Edwards, Egerer, Karpie, Karthik, Monahan, Morris, Orginos, Radyushkin, Romero, Sufian and S.Z. JHEP 03 (2023)

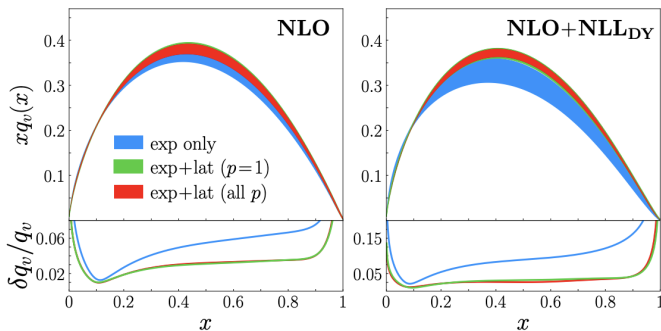
086 Real and Imaginary components of the reduced pseudo-ITD


Helicity PDF



 Edwards, Egerer, Karpie, Karthik, Morris, Orginos, Radyushkin, Romero, Sufian and S.Z. Phys.Rev.D 105 (2022) 3, 034507 The leading-twist valence helicity quark PDF (purple) and x -space contaminations compared with the recent global analyses


Complementarity of experimental and lattice QCD data on pion parton distributions



Valence quark distributions (**top**) when extracted from experimental data alone (blue), combined with the $p = 1$ lattice data (green), and combined with all the lattice data (red) for the NLO (**left**) and NLO+NLL_{DY} (**right**) cases, along with the relative uncertainties (**bottom**). The bands represent a 1σ uncertainty level.  Barry, Egerer, Karpie, Melnitchouk, Orginos, Richards, Sato, Sufian, Qiu, S.Z.

Phys.Rev.D 105 (2022) 11, 114051

Conclusions and outlook

- PDFs are needed as theoretical inputs to all hadron scattering experiments and in some cases are the largest theory uncertainty.
- The lattice community is by now able to provide ab-initio determinations of PDFs without theoretical obstructions.
- The interplay between lattice QCD and global fits is very important
- Also important in the search of New Physics  Gao, Harland-Lang, Rojo (2018)
- What next?
- **Many thanks for your attention!!!**